In situ high pressure and high temperature Raman studies of $(1-x)SiO_2 xGeO_2$ glasses

2009 J. Phys.: Condens. Matter 21 375109

(http://iopscience.iop.org/0953-8984/21/37/375109)

J. Phys.: Condens. Matter **21** (2009) 375109 (11pp) doi:10.1088/0953-8984/21/37/375109

In situ high pressure and high temperature Raman studies of $(1-x)SiO_2xGeO_2$ glasses

R Le Parc[1], V Ranieri[2], J Haines[2], M Cambon[2], O Cambon[2], C Levelut[1] and S Clément[1]

[1] Laboratoire des Colloides Verres et Nanomatériaux, UMR CNRS-UM2 5587, Université Montpellier 2, Place Eugène Bataillon, 34095 Montpellier Cedex 5, France
[2] Institut Charles Gerhardt Montpellier, Équipe PMOF, UMR CNRS-UM2 5253, Université Montpellier 2, Place Eugène Bataillon, 34095 Montpellier Cedex 5, France

Received 9 June 2009
Published 21 August 2009
Online at stacks.iop.org/JPhysCM/21/375109

Abstract
The structure of glasses in the binary system SiO_2–GeO_2 has been studied by Raman spectroscopy. Our results are consistent with mixing of SiO_2 and GeO_2 tetrahedra. The changes induced by temperature and by pressure on the structure are monitored by *in situ* measurements on the same mixed glasses. Anomalous temperature dependences are observed not only for SiO_2 glass and GeO_2 glass but also for mixed glasses. Particular attention is focused on the pressure densification mechanism in mixed glasses. Via the pressure dependence of the width of the main Raman band, we show that the compression mechanism in mixed glasses is intermediate between that of the end members.

1. Introduction

Germanosilicate glasses have been and still are the subject of considerable interest for optical applications. At low GeO_2 concentrations, they are used for standard optical fibres cores, in which phase gratings can be photo-induced. At higher GeO_2 concentrations, they can be used for Raman amplification.

Low concentration Ge-doped glasses (up to 15% molar) have been rather widely studied in order to understand the UV radiation writing mechanism [1, 2] and the influence of thermal history on their structure [3–8]. For higher germanium concentrations, some structural investigations are also reported via Raman spectroscopy [9, 10], XAS [11, 12], diffraction [13], NMR [14] and macroscopic characterization [15–17]. Whereas density and refraction index exhibit a linear composition dependence between the two end members, [15, 16], thermal expansion and glass transition temperature, T_g, do not [17, 15]. Then the question of the homogeneity of the mixed glasses is discussed [16, 18] and clustering or phase separation are suspected [17]. On the argument of the absence of a region of constant viscosity, Birtch [16] excluded phase separation and no sign of clustering or phase separation can be detected in the SAXS experiment for compositions up to 21% molar at room temperature [19]. Yet the non-ideal mixing of SiO_2–GeO_2 glasses is still discussed: non-regular tetrahedral and non-connected tetrahedral are still evoked [13].

From a fundamental point of view, mixed SiO_2–GeO_2 glasses give rise to particular interest because they mix two model glasses, which are good glass formers with completely connected tetrahedral networks. Paradoxically these 'model glasses' are also known for their anomalous behaviours versus temperature and pressure as compared to their alkali counterparts. For example, an increase of the elastic moduli of silica glass for temperatures higher than 83 K has been related to the anomalous densification with temperature [20, 21]. For germania, rather similar anomalous elastic properties are reported [22]. Both glasses also exhibit an anomalous decrease of the sound velocity for moderate pressures followed by the expected increase above 2 GPa [23].

Many high pressure studies (x-ray diffraction [24–30], Brillouin [31, 32], infrared [33, 34] and Raman spectroscopy [35–38]) have pointed out the interest in the compression mechanism in SiO_2 and GeO_2 glasses and melts and their polyamorphic nature [39, 36, 40]. As a matter of fact, both glasses exhibit at first a reversible compression regime followed by an irreversible one with increasing pressure, with recovered glasses being permanently densified. In silica glass, up to 8–10 GPa compression is associated with changes in the intermediate range order (IRO): volume reduction of voids associated with a gradual and reversible decrease of the Si–O–Si intertetrahedral (θ) angle. Above this pressure,

the compression mechanism is dominated by an increasing distortion of the tetrahedra. Changes in short range order are then observed around 10–15 GPa and the average Si coordination starts to change from 4 to (5 or) 6.

In the case of GeO_2, from 0 to 4 GPa, the dominant compression mechanism is closer packing of relatively rigid tetrahedra followed by a rotation of tetrahedra around the Ge–O–Ge linkage, leading to some distortion in bonds [28]. XAS performed around the Ge k-edge, shows that above 4–6 GPa the coordination of some Ge atoms starts to change from 4 to 6 [39, 40].

The end of the coordination change is a matter of debate for both glasses. According to a recent *in situ* x-ray diffraction study [29], Si coordination reaches 6 in the range 45–50 GPa and the glass exhibits stishovite-like local structure, at least up to 100 GPa, whereas x-ray Raman results conclude that the coordination change is not finished at 74 GPa [41]. For GeO_2, the coordination change was assumed to be complete around 13 GPa from Raman spectroscopy [38], whereas recent EXAFS results demonstrate that full octahedral state is not reached at 13 GPa [40]. An intermediate glassy form with an average coordination of around 5 is also mentioned [27, 42], but not supported by XAS and XANES [39, 40]. Therefore, it appears that if many studies converge on a secondary compression mechanism involving coordination changes in both glasses, the detailed pressure evolution of the structure is not completely clarified. Because of the initial differences in intertetrahedral angle values, the structural changes happen much earlier in GeO_2 than in SiO_2 and should also lead to interesting densification mechanisms in mixed glasses.

Raman has proven to be a relevant probe to investigate the short and intermediate range structure in glasses. This paper describes an investigation of binary glasses' structure for different compositions between SiO_2 and GeO_2. For the first time, the influence of temperature and pressure on Raman spectra of these glasses is studied *in situ*, for a better understanding of their structure. Pressure-induced modifications of Ge-rich $(1-x)SiO_2xGeO_2$ glasses is of particular interest for high Ge content optical fibres. In fact, rapid quenching of Ge-doped core (higher thermal expansion) surrounded by silica cladding (low thermal expansion) can induce high stress in the fibre core and limits the synthesis of cores containing a high percentage of GeO_2.

2. Experiment

Mixed $(1-x)SiO_2$–$xGeO_2$ samples were prepared from the melt in a platinum crucible and quenched. Pure GeO_2 from Stanford Materials Corporation (5N purity) and SiO_2 from Fluka were used. For samples containing 30 and 50% GeO_2, the powders melted at 1685 °C, while the sample containing 80% GeO_2 powder melted at 1350 °C. After a plateau at an intermediate temperature (1200–1050 °C), samples containing more than 50% GeO_2 were quenched in air.

Infrared measurements were performed with a Perkin-Elmer Spectrum-One 2000 spectrometer in a reflection mode (angle 180°). Raman measurements were performed with the T64000 Jobin-Yvon confocal micro-Raman spectrometer using a 50 × objective. The 514.532 nm line from a coherent argon ion laser was used as an excitation line.

A Linkam TS1500 heating device designed to work from 50 to 1500 °C, adapted on the spectrometer, was used for high temperature measurements. The temperature was controlled by a thermocouple at the bottom of the crucible. Measurements were performed in air through the silica windows from room temperature up to 1100 °C. Each time a new temperature was reached, the sample was stabilized for a few minutes before acquisition. The spectra at high temperature are corrected for the thermal radiation background, and the experimental spectrum was treated in order to obtain reduced intensity:

$$I\mathrm{red} = I_{\mathrm{mes}}(\omega)\frac{\omega}{(n+1)(\omega_0-\omega)^4} \quad (1)$$

where ω is the Raman shift (cm^{-1}), ω_0 is the absolute wavenumber of the laser light (19 435 cm^{-1}) and n is the Bose–Einstein factor.

The experiments at high pressure were carried out with a gas membrane diamond anvil cell (DAC) Diacell-HeliosDAC from Easylab. The gasket hole (100–120 μm) was filled with 1 or 2 small pieces of glass, ruby chips and a pressure transmitting medium. The pressure in the DAC was determined from the spectral shift of the ruby R_1 fluorescence line. Methanol or 4:1 methanol:ethanol were used as pressure transmitting media having hydrostatic limits of 8.6 GPa and of 9–10 GPa. Above 8 GPa, quasi-hydrostaticity can be estimated based on the resolution of the ruby lines. Compression was performed step by step, as was the following decompression. Finally, the spectrum of the recovered sample was also measured at room conditions.

3. Results

3.1. SiO_2GeO_2 at room pressure and temperature

Figure 1(a) shows Raman spectra for samples containing, from top to bottom, 0, 20, 30, 40, 50, 60, 80 and 100% GeO_2. Raman spectral bands for silica glass have been assigned from [43, 44]. The broad main band around 440 cm^{-1} ($\omega_1(0)$) arises largely from the motion of bridging oxygen along the Si–O–Si angle bisection and is assigned to a symmetric stretching motion of the oxygen. The cross section of this highly polarized mode arises as the vibrational displacement of the bridging oxygen associated with this mode maintains the local site symmetry of the O atom (C2v) [45]. Symmetric bending of Si–O–Si and O–Si–O deformation of the coupled tetrahedra are also mentioned for assignation of this band [46]. The width of the band $\omega_1(0)$ has been explained by the contribution of vibrations from a large distribution of ring structures of different sizes. The Si–O–Si angular distribution covers 120°–180° with a mean value around 144° [47]. The two bands around 495 and 606 cm^{-1} rise sharply out of the broad band. They are associated with vibrations arising from ring structures of four and three members, respectively, which are vibrating independently from the network.

The mode observed at 800 cm^{-1} ($\omega_3(0)$) is associated with the symmetric stretch of Si–O bond involving both Si and Ge.

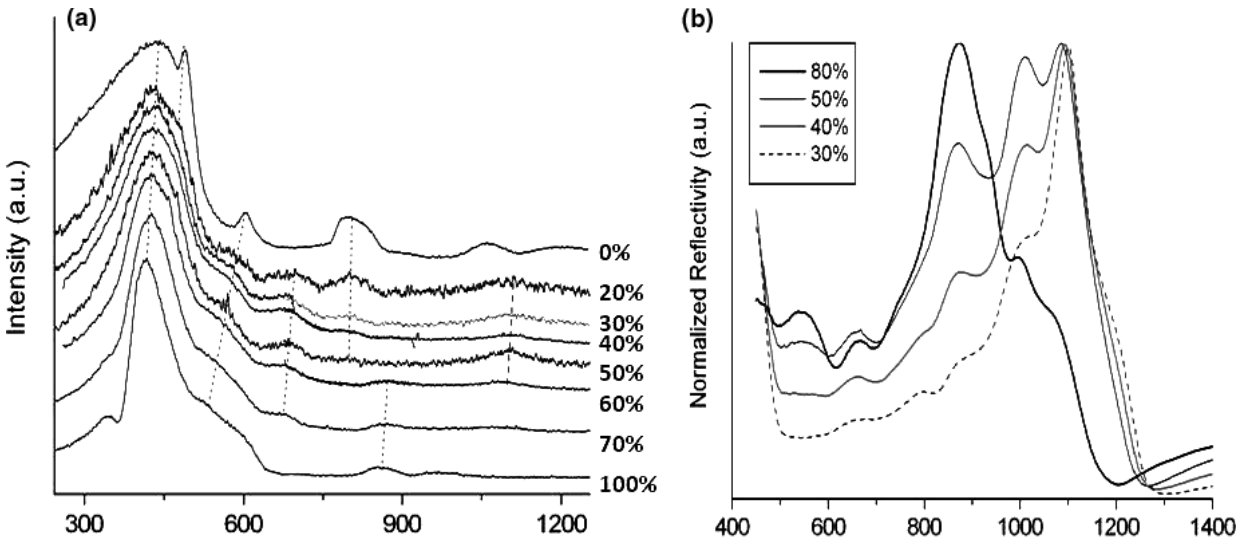

Figure 1. Raman (a) and IR reflection (b) spectra of mixed glasses for different GeO_2 contents.

Finally, the doublet at 1065–1200 cm^{-1} ($\omega_4(0)$) and ($\omega_4(0)'$) is assigned respectively to the TO and LO asymmetric stretch of Si–O.

It is quite clear that the Raman spectrum of silica glass is strongly modified when GeO_2 is added. The most important change is observed for D_1 and D_2, which broaden and disappear. For increasing GeO_2 concentration, the broad band ω_1 shifts to lower frequencies and becomes narrower, and a contribution around 340 cm^{-1} appears. Two new shoulders/bands also appear around 580 and 675 cm^{-1}.

For concentrations as high as 80%, the spectrum becomes very similar to that of GeO_2, where the band $\omega_1(100)$ at 417 cm^{-1}, corresponding to symmetric stretch of the oxygen bridging between two GeO_4 tetrahedra, is much narrower than in silica because of a smaller Ge–O–Ge angular distribution of about 10°. A small peak around 340 cm^{-1} is also observed in GeO_2 that has been associated with a vibration in which Ge motion is predominant with respect to O motion. In GeO_2, the broad shoulders around 520 and 560 cm^{-1} are respectively assigned to the mode $\omega_1(100)$ in three-membered rings (that we will name $\omega_{1R3}(100)$) and the LO–TO pair of the symmetric stretch of Ge and O in Ge–O–Ge. Finally the modes $\omega_4(100)$ and $\omega_4'(100)$ are respectively observed at 860 and 980 cm^{-1}. Table 1 summarizes the assignment and position of different bands for different compositions.

Figure 2(a) shows the influence of composition on the Raman shift of some peaks for $(1-x)SiO_2$–$xGeO_2$ glasses. The results, compared to that of Sharma [10], are in general good agreement. Some discrepancies can be explained by a different deconvolution of the curves and by a weak signal at high frequencies. The shift of the main band ω_1 is not shown on this graph, because the width and dissymmetry of this band make it difficult to give an estimation of its real position. Yet, for the band corresponding to the three-membered ring vibration $\omega_{1R3}(100)$, the position can be identified. This band shifts toward lower frequencies when germanium content increases, and this shift is 'accelerated' when germanium content increases beyond 60%. In figure 2(b), the width of the main broad band is shown to decrease progressively with GeO_2 content.

Table 1. Assignment and Raman shift for some Raman bands observed in mixed glasses.

Assignment	Sample	Designation	Position (cm^{-1})
Symmetric stretch (/bend) of TOT	SiO_2	$\omega_1(0)$	452
	30% GeO_2	$\omega_1(30)$	450
	50% GeO_2	$\omega_1(50)$	442
	80% GeO_2	$\omega_1(80)$	426
	GeO_2	$\omega_1(100)$	422
Symmetric stretch of TOT T and O moving	SiO_2	$\omega_3(0)$	800
	30% GeO_2	$\omega_3(30)$	680, 790
	50% GeO_2	$\omega_3(50)$	560, 670, 790
	80% GeO_2	$\omega_3(80)$	540, 666
	GeO_2	$\omega_3(100)$	580
Asymmetrical stretch TOT	SiO_2	$\omega_4(0)$ and $\omega_4'(0)$	1060, 1190
	30% GeO_2	$\omega_4(30)$ and $\omega_4'(30)$	880, 987, 1113
	50% GeO_2	$\omega_4(50)$ and $\omega_4'(50)$	880, 981, 1094
	80% GeO_2	$\omega_4(80)$ and $\omega_4'(80)$	866, 944, 1073
	GeO_2	$\omega_4(100)$ and $\omega_4'(100)$	860, 980

Figure 1(b) shows infrared reflectance spectra for different germanium contents. For silica glass, the main peak corresponding to the Si–O–Si antisymmetric stretch ($\omega_a(0)$) is observed around 1120 cm^{-1} [4, 7] with a shoulder around 1230 cm^{-1}. For GeO_2, the corresponding Ge–O–Ge vibration ($\omega_a(100)$) is observed around 915 cm^{-1} with a shoulder around 830 cm^{-1}. For intermediate compositions, the peak $\omega_a(0)$ is shifted to lower frequencies. The peak ω_a for the sample containing 80% GeO_2 appears as a peak at 870 cm^{-1} plus a shoulder around 930 cm^{-1}. Finally a new peak around 1010 cm^{-1} appears and increases when Ge content increases.

3.2. SiO_2GeO_2 glasses versus temperature

Figure 3 shows reduced Raman spectra for different molar compositions in GeO_2 for different temperatures in the range (20–1000 °C). Up to 50% GeO_2, very few changes are induced by temperature in the spectra apart from a progressive

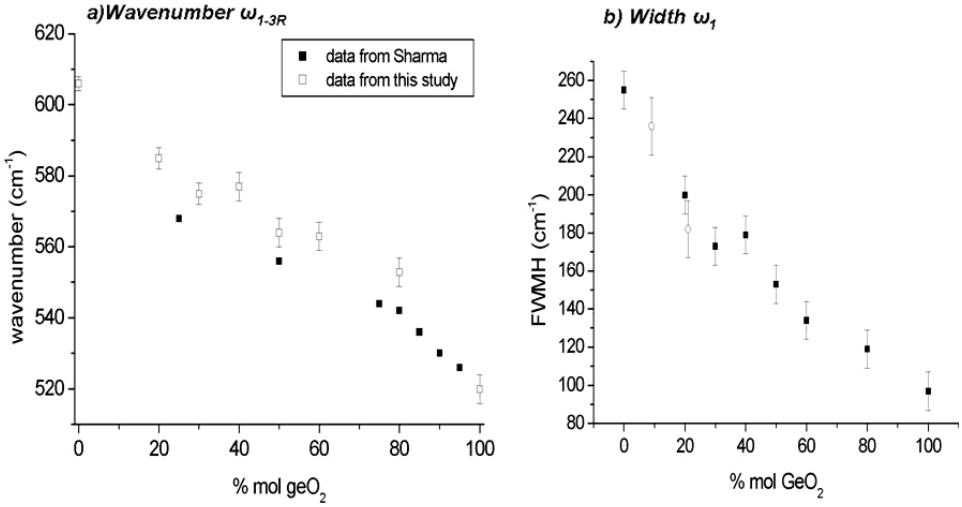

Figure 2. (a) Raman shift for ω_{1-3R} versus molar composition; data from [10] are given for comparison, (b) Raman width for ω_1 versus molar composition; full squares correspond to data from this study and open circles to data from [4].

broadening of the bands. The broadening is difficult to quantify as, for Ge-containing glasses, the smaller bands convoluting the main band seem to become more intense when temperature increases. For GeO_2-rich glasses (and GeO_2), a relative change between the main peak $\omega_1(100)$ and its shoulder at 550 cm^{-1} (ω_{13R}) is observed in the spectra and finally at the highest temperature a peak grows out of the shoulder at 530 cm^{-1}.

From figure 4 and from the extrapolation of the temperature dependence, it clearly appears that some peaks shift when temperature increases. In particular, the position for ω_1 was determined by a Gaussian fit of the top of the band in a constant wavenumber interval. This method has been previously used for studies on thermal history [4]. A small shift to higher frequencies is observed for ω_1 whereas other bands shift to lower frequencies. Bands associated with asymmetric T–O–T stretch ω_4 and ω_4' (T = Si or Ge) show an important shift in comparison with other vibrations.

The expected T_g is indicated by the end of the guiding line on figure 4. A change of slope could be expected around T_g as observed in some silicates [48]: such a change cannot be shown here within experimental error.

3.3. SiO_2GeO_2 glasses versus pressure

Figure 5 shows results for compression of samples composed of 30, 50 and 80% GeO_2. For all samples, pressure induces an obvious shift of the band ω_1 towards higher frequencies (cf figure 6(a)). This shift of the band ω_1 is continuous but not linear: the slope becomes slightly smaller above 7–8 GPa. It is particularly interesting to follow the width of the main band for these two compositions (figure 6(c)). For the sample containing 30% and 50% GeO_2, the width decreases up to 8 and 4 GPa, respectively, then from respectively 10 and 7 GPa, the peak broadens again under pressure. For the sample containing 80% GeO_2, the sharpening at low pressure is not observed at first glance within experimental error. Then the broadening is observed for pressures higher than 3–4 GPa. In figure 6(a), it appears clear that during decompression (open symbols) the main peak ω_1 keeps shifting to higher frequencies and the shifts are quite similar for all three compositions (figure 6(b)). The spectra after pressure release are different from the initial sample (figure 5): the main band is shifted to higher frequencies and is split, i.e. convoluted with a companion peak at higher frequency. The companion peak can be deconvoluted for pressures lower than 6–8 GPa for samples containing 30% and 50% GeO_2, and only at room pressure for 80% GeO_2.

4. Discussion

4.1. SiO_2GeO_2 at ambient conditions

The ambient temperature structure of $(1-x)SiO_2$–$xGeO_2$ glasses is still subject to debate. Results from Raman and IR spectroscopy can also be considered for this discussion: when the GeO_2 content increases, new peaks appear that cannot be assigned to identified Si–O–Si or Ge–O–Ge vibrations. Such a new peak is observed with Raman in the range (670–690) cm^{-1}, depending on the composition, and has been assigned to Ge–O–Si symmetric stretching [9, 10]. This peak is observed for compositions as low as 9% [4] and as high as 95% GeO_2 [9]. A new peak is also reported [9, 10] in the 980–920 cm^{-1} range assigned to Ge–O–Si asymmetric stretch. The same vibration appears in infrared measurements, giving rise to a peak around 1010 cm^{-1} for mixed compositions. The presence of fractions of three bridging oxygen species Si–O–Si, Ge–O–Ge and Si–O–Ge imply network mixing. Du [14] estimates, based on NMR results, that the proportion of the three species Si–O–Si, Ge–O–Ge, Ge–O–Si are 27, 27, 46 ± 2%, respectively, for a glass containing 50% GeO_2, which is consistent with values expected for random mixing of cations Si^{4+} and Ge^{4+} in the network. The strong modification of the D_1 and D_2 bands associated with the small three-and four-membered rings in Raman with germanium content is also clearly a sign of the introduction of germanium in the small rings. The D_1 and D_2 bands decrease in intensity

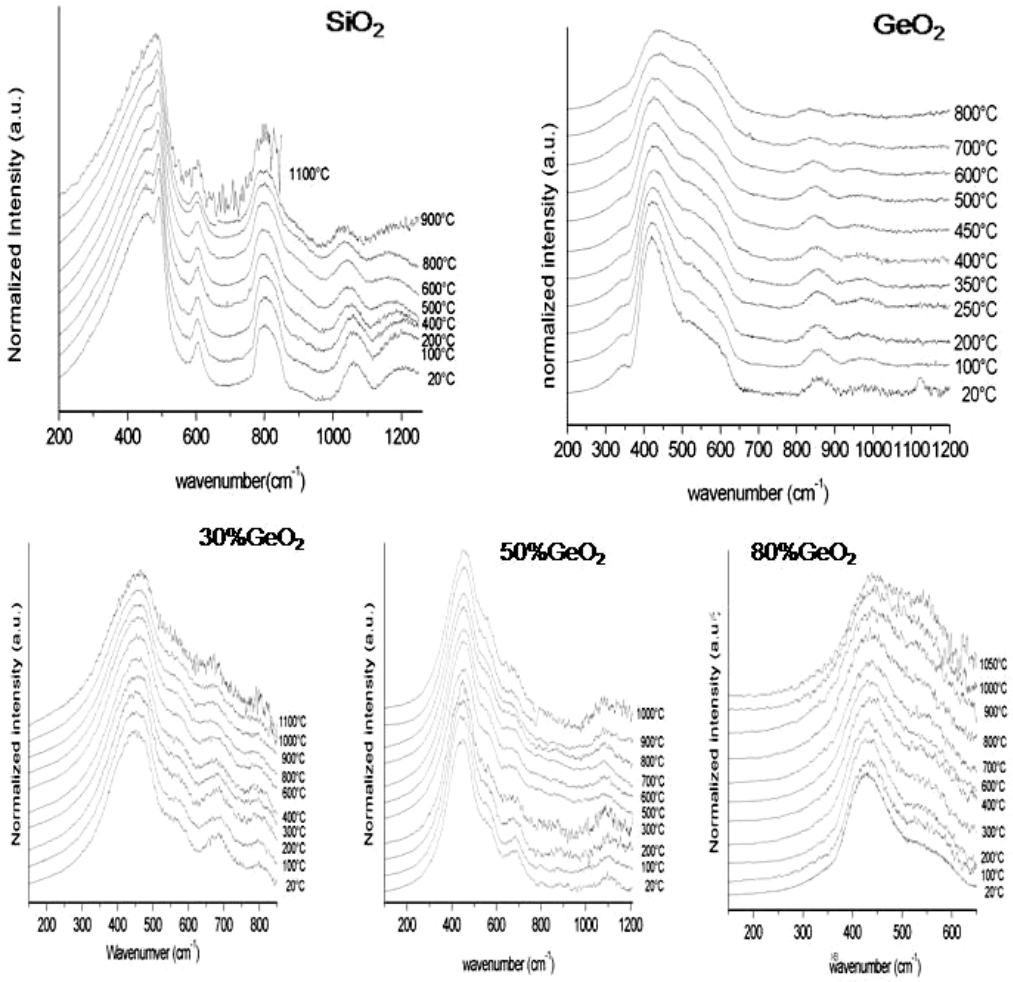

Figure 3. Evolution of reduced Raman spectra at different temperatures for a few selected mixed glasses.

due either to the disappearance of the small rings or to a progressive correlation of the vibration to the network [6, 4]. In particular, in the three-membered rings, the intertetrahedral angle is close to 130° (three members), thus corresponding to the value estimated for the mean angle Ge–O–Ge and close to that estimated for the mean Ge–O–Si (134°) in a glass containing 29% GeO_2 [13]. Henderson *et al* suggested, from Raman spectra, that mixed glasses are composed by large SiO_4, large mixed $GeO_4 + SiO_4$, large GeO_4 and small three-membered GeO_4 rings [46]. As each T–O–T contribution is well separated in IR spectra, it appears clearly here that, for a glass containing 50% GeO_2, the peak corresponding to the three T–O–T species rises strongly. The position of the Si–O–Si peak is shifted to lower frequencies by about 0.5 cm^{-1}/%mol GeO_2 when GeO_2 content increases, in agreement with previous observations [4]. This can indicate a decrease of mean Si–O–Si angle and explain the continuous FWMH reduction of the broad Raman band resulting from the three T–O–T contributions. In a more general way, with increasing GeO_2 content, the mixed glasses exhibit lower mean angles and smaller angular distributions explained by an increasing proportion of smaller angles like Ge–O–Si and Ge–O–Ge, and by a decrease of Si–O–Si angle and proportion.

Even if the agreement is good on the mixing of SiO_2 and GeO_2 tetrahedra, the ideal randomly mixed network is still debated [16, 49]. Although some measurements in quartz-type solid solutions have shown that the wavenumbers for different vibrations evolve linearly with the molar composition [50, 51], the wavenumber dependence of the peak corresponding to ω_1 and to ω_{13R} on molar composition (figure 2(b)) is not linear. A change in slope is observed around 80% GeO_2. But in the case of SiO_2–GeO_2 glasses, the nonlinearity of ω_1 position could also be explained by the strong Raman activity of Ge–O bond as compared to Si–O one. Thus the Ge–O contribution may strongly dominate that of Si–O for compositions higher than 80% GeO_2.

Thus, results from Raman and IR spectroscopy do converge for the mixing of SiO_4 and GeO_4 tetrahedra, even in small ring structures. No conclusion about a potential non-ideal mixing can be made, but a great number of non-bridging oxygens are excluded as no Raman bands associated with Q^n ($n < 3$) species around 950 or 1100 cm^{-1} for $Si–O_{NB}$ [52], and 780 or 920 cm^{-1} for $Ge–O_{NB}$ [53] are observed.

4.2. SiO_2GeO_2 glasses versus temperature

The positive Raman temperature dependence for the band $\omega_1(0)$ in silica glass, whereas the other bands have

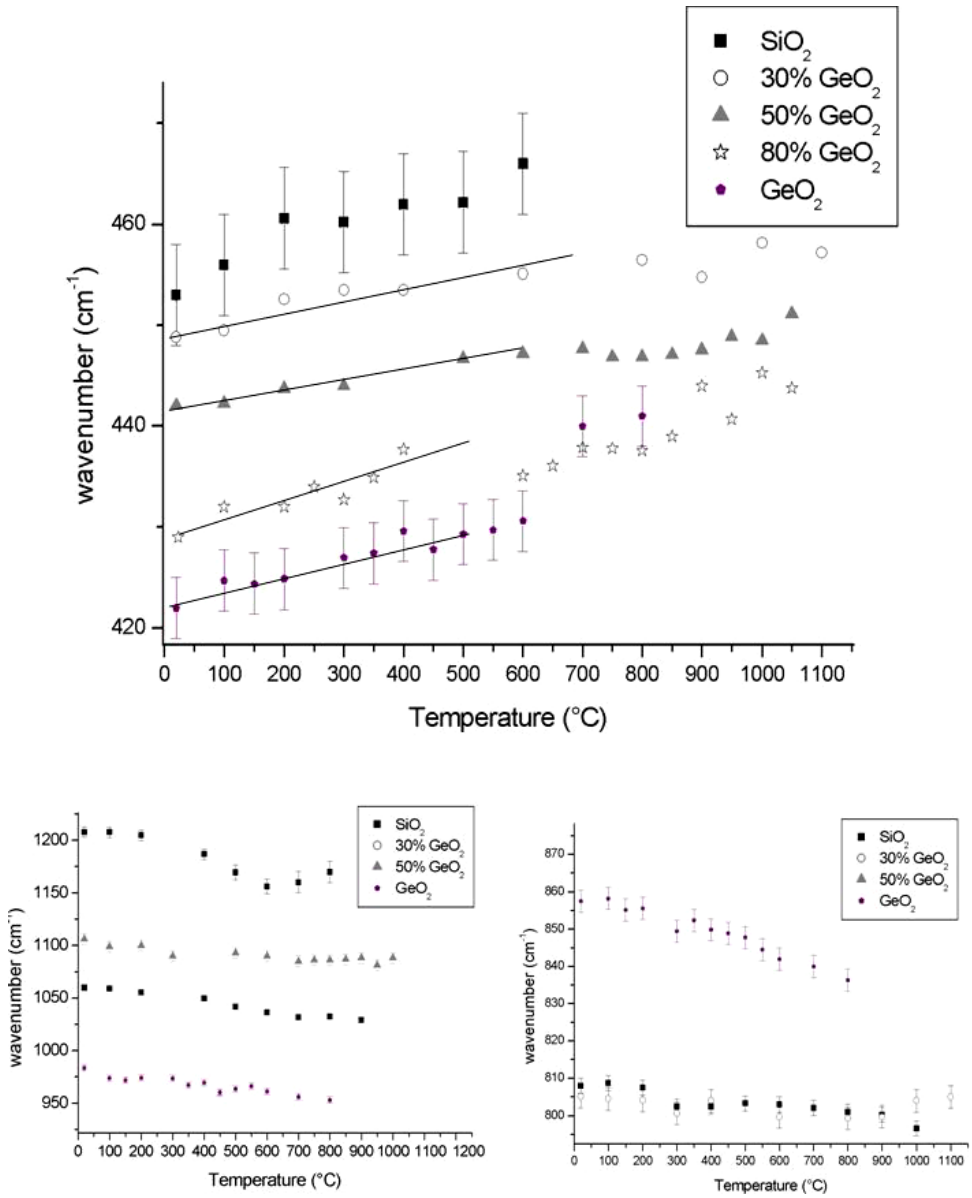

Figure 4. Raman shifts versus temperature for different mixed glasses. Lines are guides for the eyes drawn up to the expected T_g—extrapolated from [16]—1200, 700, 600, 550 and 500 °C respectively for 0, 30, 50, 80 and 100% GeO_2. For GeO_2 two points lie off the line; this corresponds to an important change in volume and the peak position is more difficult to measure.

negative temperature dependence, is consistent with results from [54–56]. In the recent study from Henderson *et al* [46], $\omega_1(0)$ remains fixed but broadens slightly, whereas $\omega_1(x > 0)$ shifts toward higher frequencies with increasing temperature. The discrepancies found for silica are explained by the possible contribution of elastic and quasi-elastic wings as a background for the main broad band [56]. The difficult determination of the mean position for the very large and asymmetric $\omega_1(0)$ band could also explain the different results for silica. The thermal dependence of ω_1 is anomalous as compared to alkali silicate glass (example: float glass) [48], for which all the vibrational bands are shifted toward lower frequencies including the band corresponding to ω_1. According to the central force network dynamic model [44, 54], $\omega_1(0)$ and $\omega_4'(0)$ frequencies can be related to the central force constant, the atomic mass for Si and O, and θ, the intertetrahedral Si–O–Si angle:

$$\omega_1(0)^2 = \frac{k}{m_0}(1 + \cos\theta) \tag{2}$$

$$\omega_4'(0)^2 = \frac{k}{m_0}(1 - \cos\theta) + \left(\frac{4k}{3m_{Si}}\right). \tag{3}$$

In order to explain the observed shifts, anharmonicity has to be considered. Average thermal expansion is expected to induce an increase of the bond length Si–O and so to decrease the force constant k. Then at first glance, anharmonicity of the vibrations is expected to induce a shift to lower frequency of both $\omega_1(0)$ and ω_4' as observed in float glass. The anomalous temperature shift observed here can be explained by the reduction of the T–O–T angle induced through ω_1

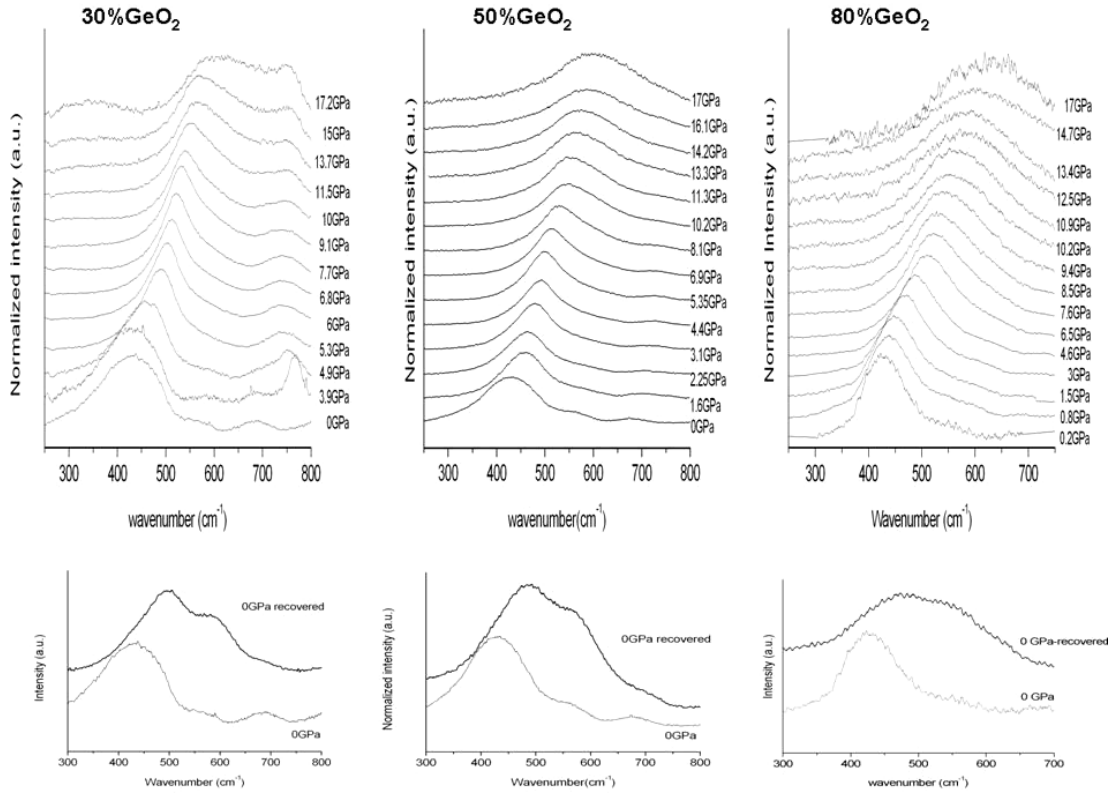

Figure 5. Evolution of Raman spectra for a few selected SiO_2–GeO_2 compositions. The broad peak observed at 775 cm^{-1} for the sample with 30% GeO_2 is due to transmitting pressure liquid. The spectra of the recovered samples are also compared to initial sample.

type vibration (the oxygen atom moves further from the Si $\cdots$ Si line, inducing a decrease in θ) [54]. This anomalous temperature shift is observed for all compositions although k would be expected to decrease with GeO_2 content. As a matter of fact, the average thermal expansion in the range 0.5–8 $\times$ 10^{-6} K^{-1} increases with the addition of germanium to silica. So the angular T–O–T reduction seems to be the dominant mechanism for any GeO_2 contents.

Even if the glass transition is not always easy to show from Raman spectra, it is important to distinguish the sub-[T_g] regime where the spectra modifications have only a dynamic nature from the glass transition and supercooled liquid range where the structural relaxation may give rise to additional modifications of Raman spectra. The changes in density fluctuation magnitude thermal dependence at T_g is a clear indication of existing structural modifications beginning in the glass transition interval [48, 19]. In silica, the structural relaxation also contributes to a positive shift to ω_1 [54] which was not observed here as the measurements did not go beyond the glass transition range (1000–1300 °C). In GeO_2, the shift is also positive but not clearly different from the sub-T_g range within the error range. As a matter of fact, a small reduction of mean T–O–T angles is expected for SiO_2 and mixed glasses from results on glasses having different thermal histories [44, 4, 5, 57, 58]. For GeO_2, the shortening of Ge–O bond could also contribute to a positive shift versus temperature [46].

The shoulder present around 520 cm^{-1} in GeO_2 glass and 80% GeO_2 shows an appreciable increase in intensity at high temperature. This band is assigned to ω_{13R} in three-membered rings, more numerous in GeO_2 than in SiO_2 [59]. This change in intensity has been interpreted by an increase of the number of planar three-membered rings in the melt as compared to the glass [46]. The changes observed this band's counterpart in silica, D_2, are a matter of discussion. Whereas McMillan *et al*'s results [54] shows a small intensity enhancement above T_g, in agreement with the enhancement measured with increasing fictive temperature [44, 57], Papatheodorou *et al* show that D_1 intensity decreases and D_2 intensity appears invariant even above T_g [60]. In this present study, in the sub-T_g regime, we find a decreasing tendency for both D_1 and D_2. The changes in these two 'defect' peak intensities are also very often interpreted by a proportional evolution of three-and four-membered-ring population, yet a dynamics simulation study has shown that D_1 can vanish with pressure on the loss of Raman activity although the associated population of four-membered rings still exists [61]. In silica and mixed glasses the three-membered rings participate to a very small part of the ring structure population (less than 5%), so a potential evolution is not representative of the glass structure evolution. In GeO_2, the number of three-membered rings containing GeO_4 tetrahedra may increase with temperature, but a quantitative analysis is not possible based only on Raman spectroscopy.

4.3. SiO_2GeO_2 glasses versus pressure

4.3.1. Compression mechanism. For all compositions, a continuous upshift is observed for the broad band ω_1 when

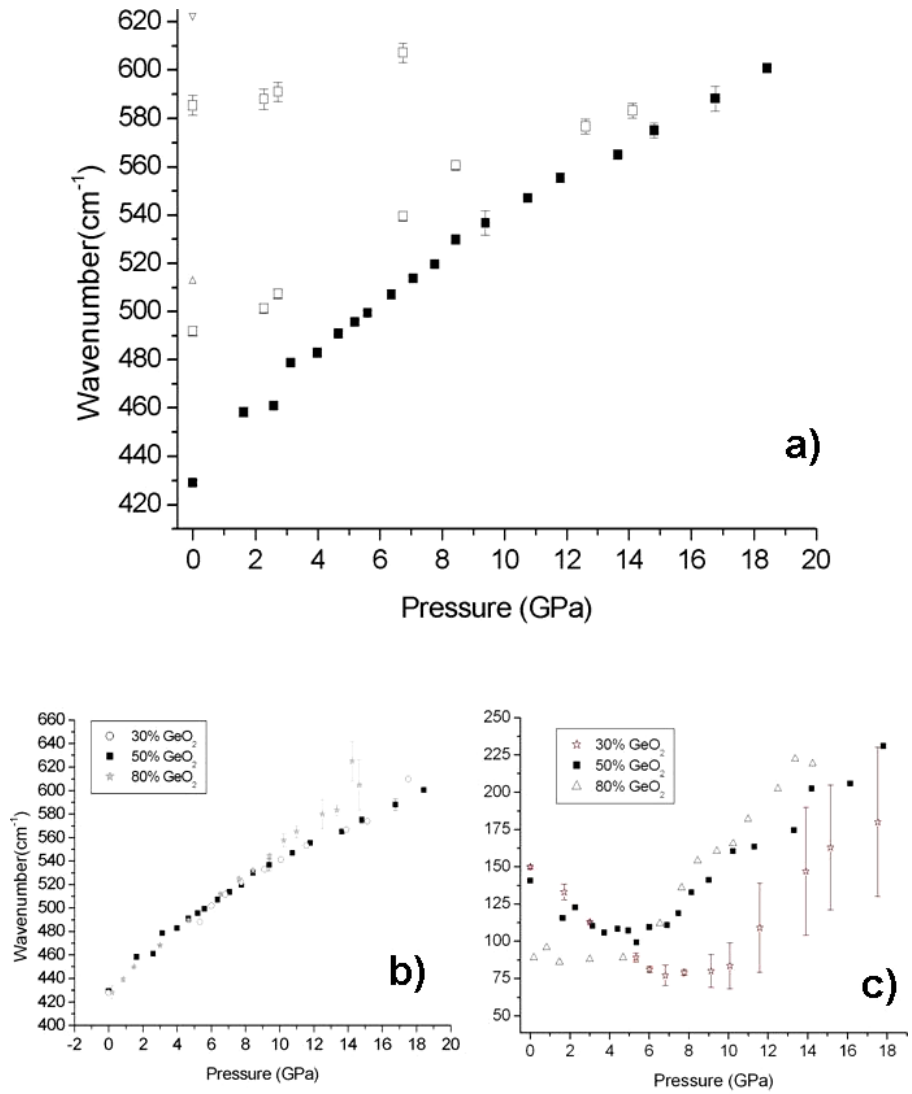

Figure 6. (a) Raman shifts for the main band during compression (full square) and decompression (open square) for a glass containing 50% GeO_2. At higher pressure, the pressure shift of the companion peak is also plotted. The two triangular points indicate the position of the main band and its companion for a sample quenched from 9 GPa. (b) The pressure dependence of the Raman shift during compression for compositions of 30, 50 and 80% GeO_2. (c) FWMH versus pressure for different GeO_2 molar composition upon compression.

pressure increases, which is consistent with measurements in SiO_2 [36] and GeO_2 [42]. Two changes in slope are observed at 4 and around 8–9 GPa. For the latter, a difference is observed for the pressure dependence of $\omega_1(30, 50)$ and that of $\omega_1(80)$. Such changes in pressure dependence of ω_1 have already been observed in silica in the 6–9 GPa range, and in GeO_2 at 2.5, 4 and 7.5 GPa [42].

A shift of ω_1 could be induced by different structural modifications in, for example, bond length, intertetrahedral angle and distortion. According to equation (2), an increase in peak position of ω_1 could be related either to a reduction in the bond length (inducing an increase of k) or to the reduction in Si–O–Si angles. Whereas simulation results show that the average Si–O distance is constant before the coordination change [61], some simulations [61, 62], some measurements [47] and interpretations provide support for the reduction of the intertetrahedral angle for compressed silica (19° at 7 GPa is found for silica [61]). Thus, if for a given pressure range, the angular reduction versus pressure is assumed to dominate over the change of k, a rough estimation of the angle for a given ω_1 can also be performed for the sample containing 30% GeO_2 using equation (2). From mean Ge–O–Ge, Ge–O–Si and Si–O–Si angles, taken as respectively equal to 130°, 134° and 144°, and their contributions varying as $2(1-x)$, $2x(1-x)$ and $2x$ respectively, then at ambient conditions mean T–O–T angles can be estimated to be 139°. We thus find an angular reduction of $10 \pm 1.5°$ up to 8 GPa for samples containing 30% GeO_2.

In fact, tetrahedral distortion is also implicated in the compressibility of the tetrahedral structures. For crystalline quartz-like structures, the tilt angle δ and the intertetrahedral θ angle are strongly linked [63] and a reduction in intertetrahedral angle induced by pressure is associated with an increase in tilt angle up to the saturation value (32°). This distortion can be detected through the decrease of Raman intensity of the ω_1 band [45]. At high pressure, the Raman

cross section of the highly polarized symmetric stretching mode ω_1 decreases strongly as the local site symmetry of the oxygen atom is modified due to tetrahedral distortion. The decrease in intensity is observed above 9 GPa in silica glass and above 3–4 GPa in GeO_2 [45] and is thus expected to start in the intermediate range for mixed glasses.

At higher pressure, the coordination change from 4 to 6 is associated with a lengthening of the T–O bond and should thus induce a progressive shift to lower frequencies. ω_1 pressure dependence shows a continuous positive slope probably as the result of a very progressive coordination change and contributions from four-, five-and six-coordinated Ge and Si.

Another spectacular modification is induced by pressure in the Raman spectra of 30% and 50% GeO_2 glasses. The main broad band $\omega_1(0)$ becomes very sharp and narrow for the first pressure points and then broadens at higher pressures (figure 6(c)) like in silica [36, 38, 45]. The case of the sample containing 80% GeO_2 closely mimics that of GeO_2, i.e. no reduction of the bandwidth can observed at low pressure and the peaks becomes broader above 4–5 GPa. The sharpening of the peak can be interpreted by a progressive reduction of the angular distribution of Si–O–Si and probably also Si–O–Ge distribution in 30 and 50% GeO_2 glasses. Like in silica, reduction/collapse of voids [25] and disappearance of a large open structure [45] as the first steps in the compression mechanism could induce a dip in a progressive reduction of Si–O–T angles. In the case of the sample containing 80% GeO_2, up to 5 GPa, the width is constant, whereas for GeO_2 the peak broadens from 3.7 GPa. For high GeO_2 contents (>80%), the angular distribution is already narrow at room temperature (about 10° around 130° in GeO_2 [38]), and the angular reduction is much more limited than in silica.

For these mixed glasses, the compression mechanisms are rendered more complex by the presence of SiO_4, GeO_4 and mixed Si–Ge tetrahedra that respond differently to the applied pressure.

From high pressures studies of α-quartz SiO_4 and GeO_4, we can assume that $\partial\delta/\partial P$ and then $\partial\theta/\partial P$ is lower for Ge–O–Ge mean angle than for Si–O–Si mean angle [63]. This explains that the reduction of Si–O–Si angular distribution and mean angle are observed from 0 to 8–9 GPa [38] whereas Ge–O–Ge angular distribution is not so easily perceptible in Raman spectra. Distortion in SiO_4 and GeO_4 tetrahedra is also suspected to participate in the compression mechanism up to a saturation value followed by coordination change beginning at a much lower pressure for Ge than for Si. Ge–O–Si angles are expected to exhibit a mean value closer to that of Ge–O–Ge [13] which reduces the angular distribution. Thus their compression mechanism is expected to be closer to that of GeO_2 tetrahedra.

The mixed glasses, depending on their composition, are then dominated either by the Si tetrahedral or by the Ge tetrahedral compression mechanism. In the glasses containing 30 and 50% GeO_2 a reduction is observed for the first pressure points showing that silica type mechanism is still observed whereas for 80% GeO_2, this mechanism is not observed any more, which is consistent with a dominant population of Ge–O–Ge and Si–O–Ge angles. The germanium coordination change is also delayed by the presence of SiO_4 tetrahedra and is observed at 11–32, 9–26 and 5–16 GPa for glasses containing 30, 50 and 80% GeO_2, respectively [12]. It is also interesting to note that the pressure range for coordination change becomes wider as SiO_2 is introduced in GeO_2. The presence of the silica tetrahedral environment gives some more degrees of flexibility for angular reduction before the species have to change coordination. The broadening of the main peak observed from 11, 8 and 5 GPa for 30, 50 and 80% GeO_2-containing glasses seems to correspond to the beginning of the coordination change. Several new species (pentahedra [42], edge-sharing tetrahedra [38]) could contribute to the main band at different frequencies and induce broadening.

4.3.2. Permanent densification. From figure 6(a), it is clear that a different path is followed by the Raman shift for the band ω_1 during compression and decompression, which is consistent with Raman measurements on silica [36]. Within experimental error, the three samples exhibit similar ω_1 shift during decompression. Even if the result of decompression is permanent densification, the final structure is not the quenched highest pressure structure. From previous studies, we know that samples recovered upon decompression have full tetrahedral networks [12]. Ge coordination returns to four during decompression in GeO_2 [39] and in mixed glasses [12]. IR experiments also demonstrate that Si returns to fourfold coordination after decompression [34]. The average position of the band ω_1 is shifted by 65 and 53 cm^{-1} in 30% and 80% GeO_2-containing glasses (figure 5). The value for ω_1 after decompression is close to that observed at the pressure just below the beginning of the coordination change process respectively at 6 ± 1 GPa and 4 ± 1 GPa for 30% and 80% GeO_2 containing glasses. The shift can be interpreted as being due to a reduction of the mean T–O–T angles in the recovered as compared to the initial sample (for example 5% reduction has been measured by NMR in 16% densified silica [47]).

Furthermore, $\omega_1(30)$, $\omega_1(50)$ and $\omega_1(80)$ for the samples recovered from decompression are convoluted with a band appearing at about 560 cm^{-1}, consistent with the strong enhancement of the ω_{13R} band observed in GeO_2 at 520 cm^{-1} [38]. This was taken as an indication of the easier formation of three-membered rings during the conversion of O^{III} back to bridging oxygen species in a still compact network. In silica glass, a shoulder is also observed near 660 cm^{-1} after decompression and an apparent enhancement of the D_2 line is observed for a glass quenched from 15 GPa. Yet, again, any quantitative conclusion from Raman scattering about ring statistics in recovered samples is quite dangerous [61]. The apparent increase of D_2 in SiO_2, GeO_2 and mixed glasses is probably enhanced by the reduction of ω_1 intensity in the recovered sample in which tetrahedra have kept some distortion [38], and not obviously related to the change in the population of three-membered rings. In some MD simulations [62] of samples recovered from 20 GPa, a shoulder is retained in the Si–O–Si distribution, which is interpreted by remnant edge-sharing tetrahedra that could also give a contribution to the broad ω_1 band.

The structure recovered from pressures as high as 17 GPa in mixed glasses is permanently densified. But at 17 GPa, a restricted part of SiO_4 tetrahedra have experienced octahedral coordination, while others still exhibit distorted tetrahedral configuration. We could expect that the recovered mixed glass consists of GeO_4, SiO_4, mixed tetrahedra that still have small distorted small T–O–T angles after the coordination recovery [62], but also SiO_4 tetrahedra that have been able to relax (larger distribution of intertetrahedral angles).

5. Conclusion

Glasses in the SiO_2–GeO_2 binary system were studied by Raman spectroscopy. These glasses are built up of a mixture of SiO_2 and GeO_2 tetrahedra, giving rise to Si–O–Ge bonds, but this mixture may not be ideal (distortion, defects and clustering (over 20% mol GeO_2) may be suspected). Mixed glasses have inherited some anomalies from their end members in their thermal dependence. The vibrational band around $\omega_1(0)$ corresponding to the asymmetric stretch of the bridging oxygen along the Si–O–Si angle bisector shows an anomalous shift toward higher frequencies even for low temperatures. This shift is the result of the reduction of an intertetrahedral angle and the strong anharmonicity of this particular vibration. Finally, under pressure mixed glasses exhibit a densification process intermediate between that of the end members. The densification involves a reduction in T–O–T angles. Three different compression mechanisms can be identified. At low pressure the broad Si–O–Si angular distribution is reduced, with the main Raman band becoming narrower. When most angles have reached a value close to that of ambient Ge–O–Ge, the angular reduction is driven by tetrahedral rotation and tetrahedral distortion. Then, the coordination number begins to change for Ge (and at higher pressure for Si) atoms from 4 to 6, seeming to give rise to a broadening of the ω_1 band. The beginning of Ge coordination change is delayed by the presence of SiO_4 tetrahedra in the glass. After compression to 16 GPa, all the samples recovered are permanently densified and their structure contains tetrahedra, which are probably distorted: the MRO structure is probably more compact, may contain smaller rings, edge sharing tetrahedra . . .: a higher number of small rings (three-membered) is suspected but cannot be confirmed by Raman.

Acknowledgment

The authors are grateful to D Maurin for technical help for infrared spectroscopy.

References

[1] Poumellec B and Kerbouche F 1996 *J. Phys. France* III **6** 1595
[2] Médjahdi K, Boukenter A, Ouerdane Y, Messina F and Cannas M 2006 *Opt. Express* **14** 5885
[3] Duverger C, Nedelec J M, Benatsou M, Bouazaoui M, Capoen B, Ferrari M and Turrell S 1999 *J. Mol. Struct.* **480** 169
[4] Le Parc R 2002 *PhD Thesis* University of Lyon 1
[5] Martinez V, Le Parc R, Martinet C and Champagnon B 2003 *Opt. Mater.* **2** 59
[6] Martinez V, Martinet C, Champagnon B and Le parc R 2004 *J. Non-Cryst. Solids* **345** 315
[7] Hong J W, Ryu S R, Tomozawa M and Chen Q 2004 *J. Non-Cryst. Solids* **349** 148
[8] Lancry M, Flammer I, Depecker C, Poumellec B, Simons D, Nouchi P and Douay M 2007 *J. Lightwave Technol.* **25** 1198
[9] Shibata N, Horigudhi M and Edahiro T 1981 *J. Non-Cryst. Solids* **45** 115
[10] Sharma S K, Matson D W and Philpotts J A 1984 *J. Non-Cryst. Solids* **68** 99
[11] Greegor R B, Lytle F W, Kotright J and Fisher-Colbrie A 1987 *J. Non-Cryst. Solids* **89** 311–25
[12] Majerus O, Cormier L, Itié J P, Galoisy L, Neuville D and Calas G 2004 *J. Non-Cryst. Solids* **345** 34
[13] Schlenz H, Neuefeind J and Rings S 2003 *J. Phys.: Condens. Matter* **15** 4919
[14] Du L S, Peng L and Stebbins J F 2007 *J. Non-Cryst. Solids* **353** 2910
[15] Huang Y, Sarkar Y A and Shultz P C 1978 *J. Non-Cryst. Solids* **27** 29
[16] Birtch E M and Shelby J E 2006 *Phys. Chem. Glasses—Eur. J. Glass. Sci. Technol.* B **47** 182
[17] Riebling E F 1968 *J. Am. Ceram. Soc.* **51** 406
[18] Lopez-Gejo F, Busso M and Pisani C 2003 *J. Phys. Chem.* B **107** 2944
[19] Le Parc R, Champagnon B, Levelut C, Martinez V, David L, Faivre A L, Flammer I, Hazemann J L and Simon J P 2008 *J. Appl. Phys.* **103** 094917
[20] Polian A, Vo-Thanh D and Richet P 2002 *Europhys. Lett.* **57** 375
[21] Le Parc R, Levelut C, Pelous J, Martinez V and Champagnon B 2006 *J. Phys.: Condens. Matter* **18** 7507
[22] Youngman R E, Kieffer J, Bass J L and Duffrene L 1997 *J. Non-Cryst. Solids* **222** 190
[23] Stebbins J F, McMillan P F and Dingwell D B 1995 *Structure, Dynamics and Properties of Silicate Melts* (*Reviews in Mineralogy* vol 32) (Washington, DC: Mineralogical Society of America)
[24] Meade C, Hemley R J and Mao H K 1992 *Phys. Rev. Lett.* **69** 1387
[25] Inamura Y, Katayama Y, Utsumi W and Funakoshi K 2004 *Phys. Rev. Lett.* **93** 015501
[26] Inamura Y, Katayama Y and Utsumi W 2007 *J. Phys.: Condens. Matter* **19** 415104
[27] Guthrie M, Tulk C A, Benmore C J, Xu J, Yarger J L, Klug D D, Tse J S, Mao H K and Hemley R J 2004 *Phys. Rev. Lett.* **93** 115502
[28] Sampath S, Benmore C J, Lantzky K M, Neuefeind J, Leinenweber K, Price D L and Yarger J L 2003 *Phys. Rev. Lett.* **90** 115502
[29] Sato T and Funamori N 2008 *Phys. Rev. Lett.* **101** 255502
[30] Funamori N and Tsuji K 2008 *Rev. Sci. Instrum.* **79** 053903
[31] Zha C S, Hemley R J, Mao H K, Duffy T S and Meade C 1994 *Phys. Rev.* B **50** 13105
[32] Grimsditch M and Bhadra R 1998 *Phys. Rev.* B **38** 7836
[33] Teredesai P V, Anderson D T, Hauser N, Lantzky K and Yarger J L 2005 *Phys. Chem. Glasses—Eur. J. Glass Sci. Technol.* B **46** 345
[34] Velde B and Couty R 1987 *J. Non-Cryst. Solids* **94** 238
[35] Hemley R J, Mao H K, Bell P M and Mysen B O 1986 *Phys. Rev. Lett.* **57** 747
[36] Champagnon B, Martinet C, Boudeulle M, Vouagner D, Coussa C, Deschamps T and Grosvalet L 2008 *J. Non-Cryst. Solids* **354** 569
[37] Rouxel T, Ji H, Hammouda T and Moréac A 2008 *Phys. Rev. Lett.* **100** 225501
[38] Durben D J and Wolf G H 1991 *Phys. Rev.* B **43** 2355
[39] Itie J P, Polian A, Calas G, Petiau J, Fontaine A and Tolentino H 1989 *Phys. Rev. Lett.* **63** 398

[40] Vaccari M, Aquilanti G, Pascarelli S and Mathon O 2009 *J. Phys.: Condens. Matter* **21** 145403
[41] Fukui H, Kanzaki M, Hiraoka N and Cai N Q 2008 *Phys. Rev.* B **78** 012203
[42] Hong X, Shen G, Prakapenka V B, Newville M, Rivers M L and Sutton S R 2007 *Phys. Rev.* B **75** 104201
[43] Bell R J and Dean P 1970 *Discuss. Faraday Soc.* **50** 55
[44] Galeener F L 1991 *Disorder in Condensed Matter Physics* ed J Blackman and J Taguena (Oxford: Oxford University Press) p 45
Galeener F L 1985 *J. Non-Cryst. Solids* **71** 373
[45] Polsky C H, Smith K H and Wolf G H 1999 *J. Non-Cryst. Solids* **248** 159
[46] Henderson G S, Neuville D R, Cochain B and Cormier L 2009 *J. Non-Cryst. Solids* **355** 468
[47] Devine R A B, Dupree R, Farnan I and Capponi J J 1987 *Phys. Rev.* B **35** 2560
[48] Levelut C, Le Parc R, Faivre A and Champagnon B 2006 *J. Non-Cryst. Solids* **352** 4495
[49] Majerus O, Cormier L, Neuville D R, Galoisy L and Calas G 2008 *J. Non-Cryst. Solids* **354** 2204
[50] Angot E, Le Parc R, Levelut C, Beaurain M, Armand P, Cambon O and Haines J 2006 *J. Phys.: Condens. Matter* **18** 4315
[51] Ranieri V, Bourgogne D, Darracq S, Cambon M, Haines J, Cambon O, Le Parc R, Levelut C, Largeteau A and Demazeau G 2009 *Phys. Rev.* B **79** 224304
[52] Wolf G H and McMillan P F 1995 *Rev. Mineral. Geochem.* **32** 247–315
[53] Henderson G S 2007 *J. Non-Cryst. Solids* **353** 1695
[54] McMillan P F, Poe B T, Gillet P and Reynard B 1994 *Geochim. Cosmochim. Acta* **58** 3653
[55] Shimodaira N, Saito K, Sekiya E H and Ikushima A J 2006 *Phys. Rev.* B **73** 214206
[56] Kalampounias A G, Yannopoulos S N and Papatheodorou G N 2006 *J. Chem. Phys.* **124** 014504
[57] Champagnon B, Le Parc R and Guenot P 2002 *Phil. Mag.* B **82** 251
[58] Gross T M and Tomozawa M 2007 *J. Non-Cryst. Solids* **353** 4762
[59] Giacomazzi L and Pasquarello A 2007 *J. Phys.: Condens. Matter* **19** 415112
[60] Papatheodorou G N and Kalampounias A G 2009 *J. Phys.: Condens. Matter* **21** 205101
[61] Rahmani A, Benoit M and Benoit C 2003 *Phys. Rev.* B **68** 184202
[62] Tse J S, Klug D D and Le Page Y 1992 *Phys. Rev.* B **46** 5933
[63] Haines J and Cambon O 2004 *Z. Kristallogr.* **219** 314